The C. elegans HP1 homologue HPL-2 and the LIN-13 zinc finger protein form a complex implicated in vulval development.

Vincent Coustham, Cécile Bedet, Karine Monier, Sonia Schott, Marianthi Karali, Francesca Palladino

The *C. elegans* HP1 homologue HPL-2 and the LIN-13 zinc finger protein form a complex implicated in vulval development

Coustham, V., Bedet, C., Monier, K., Schott, S., Karali M., Simonet, T., and Palladino, F.
Laboratoire de Biologie Moleculaire de la Cellule, Ecole Normale Supérieure de Lyon, 46 allée d'Italie, 69007 Lyon, France.

Keywords : C. elegans, HP1, vulva

7790 words

Summary

HP1 proteins are essential components of heterochromatin and contribute to the transcriptional repression of euchromatic genes via the recruitment to specific promoters by co-repressor proteins including TIF1 and Rb. The *C. elegans* HP1 homologue HPL-2 acts in the "synMuv" (synthetic multivulval) pathway of vulval development. synMuv genes fall into three classes, named A, B and C, that define redundant negative regulators of a Ras signaling pathway required for vulval induction. Several synMuv genes encode homologues of conserved chromatin-associated proteins involved in transcriptional repression, including Rb and components of the Mi-2/NuRD and TIP60/NuA4 chromatin remodeling complexes. More recently, synMuvB genes have also been implicated in maintaining somatic cell fate specification. The available data is consistent with at least some synMuv proteins functioning together in transcription regulatory complexes. Here we show that HPL-2 physically interacts in vitro and in vivo with the multiple zinc finger protein LIN-13, another member of the synMuvB pathway. This physical interaction is mediated by a conserved motif found in many HP1-interacting proteins, and by the CSD of HPL-2. In vivo localization studies show that in embryos, HPL-2 and LIN-13 co-localize in nuclear foci. Furthermore, HPL-2 foci are lost in *lin-13* depleted embryos, demonstrating that LIN-13 is involved in HPL-2 recruitment. Our data suggests that the LIN-13/HPL-2 complex may provide a direct physical link between the Rb-related synMuvB complex and chromatin.

Introduction

HP1 proteins are a highly conserved family of proteins which directly contribute to the higher-order packaging of chromatin by binding to modified histones (Li et al., 2002). All HP1 proteins are structurally related and characterized by the presence of two conserved domains, an N-terminal chromo domain (CD) separated by a variable hinge region from a C-terminal related domain termed the chromo shadow domain (CSD). The CD is responsible for binding to methylated histone H3, while the CSD is required for dimerization and most protein-protein interactions within the nucleus (Eissenberg, 2001). Many of these interactions play an important role in directing heterochromatin formation and/or gene silencing. A large number of the CSD interaction partners contain a PXVXL pentapeptide motif, including the transcription intermediary factor TIF1, the TBP-associated factor TAFII130, and the large subunit of chromatin assembly factor 1 (CAF-1) (Le Douarin et al., 1996; Murzina et al., 1999; Vassallo and Tanese, 2002). These results suggest that HP1 proteins function as adapters, bringing together different proteins in multiprotein complexes via protein–protein interactions with the CD and CSD. The multiple interactions of the CSD underscore the complexity of HP1 dynamics. However, it remains to be established how many partners HP1 has under a given set of conditions and how important these interactions are in different cellular contexts. We previously showed by RNAi that the *C. elegans* HP1-like protein HPL-2 contributes to vulval development by acting in the Rb related synMuvB pathway antagonistic to the Ras-mediated signal transduction pathway responsible for vulval cell fate determination (Couteau et al., 2002). In addition to

2

LIN-35Rb, synMuvB genes encode homologues of the class I histone deacetylase HDA-1, EFL-1/E2F, DPL-1/DP (Ceol and Horvitz, 2001; Lu and Horvitz, 1998), and counterparts of the NuRD nucleosome remodeling and histone deacetylase complex (Solari and Ahringer, 2000; von Zelewsky et al., 2000). Based on the identity of the cloned class B synMuv genes, it has been proposed that they remodel chromatin and repress transcription of genes important for vulval cell fate specification (Lu and Horvitz, 1998; von Zelewsky et al., 2000). More recently, a TIP60/NuA4-like complex was also implicated in the negative regulation of Ras signaling during vulval cell fate specification (Ceol and Horvitz, 2004). These results strongly suggest that different chromatin remodeling and modification complexes may cooperate in the same developmental pathway. To gain insight into the specific role played by HPL-2 in vulval cell fate determination we carried out a two-hybrid screen to identify potential partners. One of the proteins identified is the LIN-13 zinc finger protein, another member of the synMuvB pathway (Ferguson and Horvitz, 1989; Thomas et al., 2003). The interaction between the two proteins was confirmed in vivo and depends on the CSD of HPL-2 and a conserved HP1 binding motif in the N-terminus of LIN-13. Finally, we show that the localization of HPL-2 in nuclear foci is completely dependent on *lin-13*. Interestingly, while inactivation of other synMuvB genes, including *lin-35* and *lin-9*, had no effect on HPL-2 localization, inactivation of *lin-15B* decreased the number and intensity of HPL-2 foci detected. Altogether, these results suggest the existence of a hierarchy in the recruitment of the synMuvB complex to chromatin.

Materials and methods

Yeast strains and media. Strains used are the following: CG1945 *(MATa gal4-542 gal80-538 ade2-101 his3-200 leu2-3,-112 trp1-901 ura3-52 lys2-801 [URA3::GAL4 17mers (X3)-CyC1TATA-lacZ] LYS2::GAL1UAS-GAL1TATA-HIS3 CYH^R)* (gift from L. Segalat); Y187 *(MATα gal4Δ gal480Δ ade2-101 his3 leu2-3,112 trp1-901 ura3-52 URA3::UASGAL1-lacZ met⁻)*; and PJ69-4a/α *(MATA/α trp-1-901 leu2-3,112 ura3-52 his3-200 gal4Δ gal480Δ LYS2 ::GAL1-HIS3 GAL2-ADE2 met2::GAL7-lacZ.* Basic methodology for yeast was as described by Fink (1991)

***C. elegans* strains and genetics.** Strains were maintained according to the standard protocol (Brenner, 1974). The following mutant alleles were used: LGI *lin-35(n745)*; LGIII *hpl-2(ok916), hpl-2(ok917), hpl-2(tm1489), lin-13(n388), unc-32(e189), unc-49(e407), dpy-17(e164)*; X *lin-15(n767). ok916, ok917* and *tm1489* alleles were backcrossed four times prior to analysis and the presence of the deletion allele confirmed by PCR analysis. The *hpl-2* wild-type sequence fully rescued synMuv and synthetic lethal phenotypes, and partially rescued the sterility of all three alleles. For expression studies *lin-39*::GFP (gift from A. Hajnal), qIs56[*lag-2*::GFP] and qIs19[*lag-2*::GFP] were used. To construct the *lin-13(n388)dpy-17(e164)hpl-2(tm1489)unc-49(e407)* strain, *lin-13(n388)/unc-32(e189)* worms were crossed with *dpy-17(e164);lin15(n767)* males and recombinant heterozygous *lin-13(n388)dpy-17(e164);lin15(n767)* were selected based on the Muv phenotype in their progeny at 20°C. Heterozygotes were then crossed with *unc-49(e407)hpl-2(tm1489)* males and *lin-13(n388) dpy-17(e164) hpl-2(tm1489) unc-49(e407)* recombinants

selected as Dpy Unc animals segregating in their progeny at 20°C. Loss of the *lin15(n767)* allele was confirmed by duplex PCR (M. Koelle lab protocol) using the following primers : for 5'-GGGAAGGTTACGTCGAACAC-3'; rev1 5'-GATTCGTCGATGGAGGCACC-3' ; rev2 5'-GCCTCGTCGGCAATTGAATG-3'. The presence of the *tm1489* deletion in *lin-13 hpl-2* mutants was confirmed by duplex PCR using the following primers: for1 (outside deletion) 5'-TACATGCAACAAACCGCGCT-3'; for2 (inside deletion) 5'-GACAGTATAAGTTCCCCGAC-3'; rev 5'-GTTTACCAGCTTTTCCGTGTG-3', followed by sequencing using both outside primers described below. The presence of the *lin-13(n388)* C to T substitution was confirmed by sequencing.

Two-hybrid screen. The full length *hpl-2a* cDNA was subcloned into plasmid pAS2.1 (Clontech) to create pCV1. The two-hybrid screen was performed by mating, as described (Fromont-Racine et al., 1997) using yeast strains CG1945 and Y187 and the *C. elegans* cDNA library λACT-RB2 (Elledge et al., 1991; Durfee et al., 1993). Positive interactions were selected using the *lacZ* and *HIS3* reporter genes on HIS selection plates supplemented with 10mM 3-AT. Interacting partners were reconfirmed by re-transformation in PJ69-4a, mating with a PJ69-4α carrying either pAS2.1 or pCV1 vectors, and selection for expression of *ADE2* and *HIS3* reporters. For directed two-hybrid assays, baits were transformed in PJ69-4α strain and mated with strain PJ69-4a carrying preys cloned in the pGADT7 vector (Clontech).

PCR of *hpl-2* fragments. For domain mapping experiments, specific fragments of *hpl-2a* cDNA sequence were amplified by PCR with oligonucleotides designed at following positions: CD, for 5'-ATGTCGAGCAAATCAACAAA-3', rev 5'-CTCAAACTCGTCCAACATCTC-3'; CSD, for 5'-GAAACGAATCAAAATGACAAATTC-3', rev 5'-TTAAAGCTCGTCGGCTTTTGG-3'; Hinge, for 5'-AGGGAATTTTCAAAGAGAGAG-3', rev 5'-CTTCTTTTCATCTTTATCCTCTTC-3'; Hinge + CSD, for 5'-AGGGAATTTTCAAAGAGAGAG-3', rev 5' -TTAAAGCTCGTCGGCTTTTGG-3'. For HPL-2Δ, primers used were for 5'- ATGTCGAGCAAATCAACAAA-3', rev 5'-ACTGTTCACCTCCTTCGCTGG-3'. For this last construct, a stop codon was added at nucleotide position 453, corresponding to the 5' breakpoint of *ok916* and *ok917* deletion alleles. For LIN-13, point mutations were introduced resulting in a change at position 442 (V to D) and position 444 (V to E) using the Quickchange Site-directed Mutagenesis kit (Stratagene) on the cDNA isolated from two-hybrid experiment. Primers used were 5'-GAACCATTCTTGTCAACCGTTGGATCC GGAGGTTGCTTACTTCCCAAAACCG-3' and 5'-CGGTTTTGGGAAGTAAGCAACCTCCGG ATCCAACGGTTGACAAGAATGGTTC-3'. The presence of the point mutations was confirmed by sequencing.

Deletion mapping. Total genomic DNA was extracted from mixed-stage populations of *ok916* and *ok917* mutant worms. Oligonucleotides were designed as described by the *C. elegans* Knockout Consortium. Nested PCR was performed using BIO-X-ACT polymerase (Bioline). The *tm1489* deletion predicted by the National BioResource Project was confirmed by sequencing using primers described below.

Reverse transcriptase-polymerase chain reaction (RT-PCR) and sequencing. Total RNA was isolated from mixed-stage populations of homozygous ok916, ok917 and N2 worms using Trizol reagent (Sigma). First-strand synthesis and RT-PCR were performed in a single reaction using the Access RT-PCR Kit (Promega). Oligonucleotides were designed at the following positions: 4799-4819 (for exon 2, 5'-AGGACAACGTGTTCATGGTGG-3'); 7011-7030 (rev exon 5-2B, 5'-CTTCAGTCATCTCAACGTCC-3'); 7617-7638 (rev exon 6-2B, 5'-ATCATCGTCTGGTACAGTG TCG-3')

RNAi. RNAi and feeding injection experiments were carried out as described (Fire et al., 1998; Kamath and Ahringer, 2003). RNAi Feeding clones were obtained from Geneservice. To produce a weaker RNAi effect, the concentration of IPTG in feeding plates was reduced to 0,1mM IPTG. Induction was 12h at room temperature. lin-15A and lin-15B-specific RNAs for injection were prepared as previously described (von Zelewsky et al., 2000). Embryos for hpl-2::GFP localization studies were dissected from gravid mothers derived either from L1 larvae grown on RNAi feeding plates, or from injected L4 larvae.

GST-pulldown assay. GST-HPL-2 fusion protein expressed in E. coli using the full-length hpl-2a cDNA cloned in pGEX-KG (Pharmacia) was immobilized on gluthatione-agarose beads (Sigma). Proteins subcloned in pGADT7 vector were produced and labeled with [35S]methionine using the TNT T7-coupled reticulocyte lysate system (Promega). Beads were incubated with in vitro produced proteins 2 hours at 4°C in PBS with 0,05-0,2% Triton, washed and analysed on SDS-PAGE.

Preparation of Embryo Extracts. Hermaphrodites carrying a rescuing LIN-13::GFP transgene were grown in liquid as described (Mains and McGhee, 1999). Embryos recovered following alkaline hypochlorite treatment of gravid adults were recovered by centrifugation, resuspended in 5 volumes of cold TNT buffer (Tris.HCl 50mM pH=8; NaCl 150mM; Triton X-100 1% + protease inhibitor cocktail (Complete EDTA, Roche Applied Science, plus 1mM PMSF) and sonicated on ice. Lysates were spun at high speed for 10 min at 4°C and supernatants were collected and assayed for protein concentration using Bradford reagent (Bio-Rad Laboratories). Protein concentration of the LIN-13::GFP embryonic lysate was $\approx$ 5mg/ml.

Immunoprecipitation and Western Blot. 3 μl of rabbit polyclonal affinity purified anti-HPL-2 antibody or preimmune serum, or 4 μg of anti-GFP (Clones 7.1&13.1, Roche Applied Science) or anti-FLAG (M2 monoclonal, Sigma) antibodies were added to 250 μl of LIN-13::GFP embryonic lysate diluted twice in TNT buffer. Samples were incubated at 4°C for 1h30 and 50 μl of a 1:1 slurry of Protein A-sepharose (Amersham Bioscience) or Protein G-sepharose (Sigma) beads were added. Samples were incubated another 2 hours at 4°C. The beads were washed two times in 1 ml of buffer A (10mM Tris.HCl pH=8; 150 mM NaCl; 0,5% T X-100), two times in 1 ml of buffer B (10mM Tris.HCl pH=8; 500 mM NaCl; 0,5% T X-100), and one time in 1ml of buffer C (10mM Tris.HCl pH=8). Proteins were resolved by SDS-PAGE followed by Western blot analysis. Primary antibodies were rabbit affinity purified anti-HPL-2 developed in the lab and diluted at 1:2000, or anti-GFP (Roche) diluted at 1:1000. Secondary antibodies were ImmunoPure Recomb Protein A-Peroxidase Conjugated (1:15 000, Pierce) or an anti-mouse IgG (from sheep) conjugated to peroxidase (1:10

000; Amersham Bioscience). Proteins were visualized using a chemiluminescent reagent kit (Super Signal, Pierce)

Construction of *hpl-2*::RFP. *hpl-2*::RFP was constructed by replacing the GFP insertion in pFG2 (Couteau et al., 2002) with a monomeric rfp fragment from pRSET B (Invitrogen). Transgenic worms were generated as described previously (Mello et al., 1991). For colocalization experiments, *hpl-2*::RFP and a rescuing *lin-13*::GFP construct (gift of I. Greenwald) were co-injected with pRF4 to generate transgenic worms.

Immunofluorescence experiments

Embryos were freeze-cracked and fixed with MetOH followed by 3% paraformaldehyde at RT. Incubation was with anti-GFP mouse monoclonal antibody (Roche) and anti-H3K9Me3 rabbit polyclonal antibody (Upstate), both diluted at 1/500. Images were acquired using a Zeiss LSM510 confocal microscope and LSM510 v3.2 software.

HPL-2-GFP acquisition, restoration and analysis. Number of nuclear HPL-2-GFP foci were counted in nuclei of live embryos fed or micro-injected with RNAi against different synMuv genes. To facilitate comparison, analyses were restricted to HPL-2-GFP embryos containing between 50-80 cells. Parameters of image acquisition, restoration and analysis were kept constant for embryos issued of various genetic backgrounds. Briefly, image stacks of whole HPL-2-GFP embryos were acquired every 0.3 μm, using the 63x objective lens (NA=1.4) of a motorized Zeiss Axioplan2 fluorescence microscope, equipped with a Coolsnap HQ camera, driven by Metamorph (v. 6.3). The 3D point spread function of our system was measured to restore image stacks using a 3D deconvolution procedure (set up with default parameters),available as a plugin in Metamorph. Maximum intensity projections of deconvolved sections were performed and observed with the same dynamic display to count nuclear foci. Superimposed nuclei as well as nuclei, which could not be visualized under those conditions (likely due to photobleaching), were not included in the analysis. In practice, approximately half of the nuclei revealed to be suitable for counting nuclear foci in the majority of embryos. The same individual counted the number of nuclear HPL-2-GFP foci in 32 to 250 nuclei for each genetic background issued from 1 to 8 representative embryos. A statistical analysis based on a one-way analysis of variance and Tukey multiple comparisons of mean differences allowed determining statistical difference between a given genetic background and the wild-type at significance $p < 0.01$ and $p < 0.001$ (Figure 6).

Reporter gene expression analysis. *lin-39*::GFP and *lag-2*::GFP strains were crossed with *unc49*(e407)*hpl-2*(ok917), *unc49*(e407)*hpl-2*(tm1489) mutants, or placed on *lin-13*(RNAi) feeding plates.

Results

HPL-2 interacts with the LIN-13 zinc finger protein in vitro and in vivo

The *hpl-2* gene gives rise to two alternatively spliced transcripts, of which only one, *hpl-2a*, contains the conserved full length CD and CSD domains (Fig. 3A,B; Couteau et al., 2002); in all studies described here *hpl-2* refers to the *hpl-2a* transcript only. We have previously shown that *hpl-2* encodes a ubiquitously

expressed protein required for germline differentiation and vulval development (Couteau et al., 2002). Given that HP1 family proteins have been shown to interact with a number of nuclear factors (Eissenberg and Elgin, 2000; Li et al., 2002), the specificity of action of HPL-2 in germline and somatic development is likely to be due to interaction with specific proteins. To identify potential partners of HPL-2, a yeast two-hybrid screen was carried out. The bait used was composed of the full-length HPL-2 protein fused to the GAL-4 DNA binding domain (DB-HPL-2). Dimerization via the CSD has been shown to be required for HP1 to interact with at least a subset of proteins (Brasher et al., 2000; Thiru et al., 2004). To ask whether HPL-2 can dimerize, DB-HPL-2 and AD-HPL-2 fusion proteins were expressed in PJ69-4a and PJ69-4α yeast strains respectively, and interaction was tested by mating. In the presence of both fusion proteins, *HIS3* and *ADE2* reporter genes were activated (Fig. 1A). This result was confirmed in an in vitro GST-pulldown assay, using a purified recombinant N-terminally epitope tagged GST-HPL-2 and an in vitro translated ^{35}S-HPL-2 (Fig. 1B). We conclude that the self-dimerization property of HP1 family proteins is conserved in *C. elegans*. The DB-HPL-2 fusion protein was then used as a bait to screen a random primed *C. elegans* cDNA bank (kind gift from R. Barstead). Out of 4.8×10^7 transformants screened, we isolated one clone encoding a fragment of *lin-13*, a member of the LIN-35Rb class of genes involved in vulval development (Ferguson and Horvitz, 1989; Thomas et al., 2003). The LIN-13 protein is characterized by 24 zinc fingers of the C2-H2 class and a LXCXE Rb binding motif (Melendez and Greenwald, 2000). The clone isolated, in frame with the GAL-4-AD domain, contains residues 173 to 909 of the protein, including the LXCXE motif and the first five zinc fingers (Fig. 1C). Interaction was validated by re-transformation of both interactors in strains PJ69-4a and PJ69-4α, mating and testing reporter gene activity (Fig. 1A). To confirm the interaction, we performed binding studies using a GST-tagged HPL-2 protein and in vitro translated ^{35}S-LIN-13 protein in a GST-pulldown assay (Fig. 1B). ^{35}S-LIN-13 was retained on GST-HPL-2 but not GST-only resin, confirming the specificity of the two-hybrid interaction. We next asked if HPL-2 and LIN-13 also associate in vivo in *C. elegans*. To this end, we performed immunoprecipitation (IP) experiments from extracts expressing a functional LIN-13::GFP fusion protein using either GFP or HPL-2 specific antibodies, followed by Western blot analysis of the resulting immunocomplexes. As shown in Fig. 1D, we found that HPL-2 antibodies efficiently co-immunoprecipitated LIN-13::GFP from these extracts. Conversely, GFP antibodies directed against LIN-13::GFP were able to co-immunoprecipitate HPL-2. Neither HPL-2 nor LIN-13::GFP could be precipitated by non-specific antibodies. Therefore, the HPL-2/LIN-13 interaction observed in vitro is also found in vivo.

The CSD and Hinge region of HPL-2 are required for interaction with LIN-13 via a PLVPV HP1 consensus motif

For most known HP1 interacting proteins, association with HP1 involves the CSD (Lechner et al., 2000; Lechner et al., 2005; Linder et al., 2001; Murzina et al., 1999; Nakayama et al., 2001; Vassallo and Tanese, 2002). To define the region of HPL-2 required for interaction with LIN-13, we performed binding studies

with in vitro translated proteins deleted for the different domains of HPL-2. We tested CD alone, hinge (H) alone, H+CSD, and CSD alone (Fig. 2A and B). While the CSD alone was sufficient for interaction with LIN-13, this interaction was approximately 10-fold stronger when the hinge region was also included, as quantified by ImageQuant. Neither the hinge region, nor the CD alone were able to interact with LIN-13. These results indicate that the CSD is essential for the interaction with LIN-13, and that amino acids present in the variable hinge region may contribute to this interaction. Since the CSD of HP1 proteins often interacts with a conserved pentapeptide motif PXVXL, we tested whether a PLVPV motif present in the N-terminal portion of LIN-13 included in the two-hybrid clone (Fig. 1C) is responsible for the interaction with HPL-2. We used site directed mutagenesis to change the conserved amino acids Val-442 and Val-444 to Asp (D) and Glu (E), respectively, to create AD-LIN-13[PLDPE]. Substitution of these amino acids significantly reduced the interaction between HP1 and TAF$_{II}$130 (Vassallo and Tanese, 2002). After verifying the expression of the LIN-13[PLDPE] mutant protein by Western blot analysis (data not shown), we tested its interaction with HPL-2 in the yeast two-hybrid system. As shown in Fig. 2C, the interaction of LIN-13 with HPL-2 was lost when the PLVPV sequence was mutated. Altogether, these results show that HPL-2 shares interaction properties with its homologues in other species.

Deletion of conserved residues within the CSD abolishes HPL-2 homodimerization but not interaction with LIN-13

Two *hpl-2* deletion mutants, *ok916* and *ok917*, were isolated by the *C. elegans* Knockout Consortium. A third deletion allele, *tm1489*, was isolated by the National BioResource Project. Although all three are deletions within the *hpl-2* coding sequence, we observed that at 25°C *ok916* animals appear generally healthier than *ok917* and *tm1489* mutant animals, suggesting that these may not all be null alleles. We therefore mapped the extent of the deletion in these alleles by sequencing the entire *hpl-2* coding sequence from homozygous mutant animals. *ok916* is a 1739 base pair (bp) deletion. RT-PCR analysis on total RNA from *ok916* mutant animals showed that this deletion results in the splicing of exon 3 to a cryptic splice donor site within exon 6, creating an open reading frame of 167 amino acids (aa) (Fig. 3A). *ok917* is a smaller deletion of 779 bp which results in the joining of exon 3 to exon 5 of *hpl-2b*. Sequence analysis showed that this mutation results in an open reading frame of 171 aa. The region deleted in *ok916* and *ok917* alleles includes conserved residues within the CSD domain (Fig. 3B,C). To study the potential effect of the loss of this region on the ability of HPL-2 to dimerize and interact with LIN-13, we inserted a stop codon after nucleotide position 453 within the *hpl-2* sequence, corresponding to the 5' breakpoint of the *ok916* and *ok917* deletion alleles. This resulted in DB- and AD-tagged HPL-2 proteins with a partially deleted CSD. Following western blot analysis to confirm expression of these truncated proteins in yeast (data not shown), two-hybrid assays were performed to test their ability to homodimerize and interact with LIN-13. Surprisingly, we found that although the truncated protein was unable to homodimerize, it maintained the ability to interact with LIN-13 when assayed on SC minus histidine plus 1mM 3-AT (Fig. 4), but not on

higher concentrations of 3-AT or on SC minus adenine, suggesting that the interaction is nonetheless weaker compared to full-length HPL-2. These results suggest that while the CSD residues missing in the *ok916* and *ok917* deletion alleles are essential for dimerization, they may not be absolutely required for the interaction of HPL-2 with the PLVPV motif of LIN-13. Sequencing of the *tm1489* allele confirmed that it is a deletion which starts 58 nucleotides upstream of the ATG and takes out the entire first and second exons, including sequences coding for the CD (Fig. 3A). This deletion is a clear molecular null allele, consistent with the observed phenotype, as described below.

hpl-2 and lin-13 genetically interact with the synMuv pathway of vulval development

All three *hpl-2* mutant alleles show phenotypes similar to those we previously reported for *hpl-2*(RNAi) animals, including sterility, slow growth and an everted vulva (evl, Table 1A) (Couteau et al., 2002). However, the penetrance of these phenotypes appeared to be higher for the *ok917* and *tm1489* alleles, which at 25°C were also thin and scrawny and showed additional defects in vulva development. These data are consistent with the molecular analysis suggesting that *ok916* and perhaps *ok917* are not null alleles.

In *C. elegans*, the vulva is derived from three of the six equivalent vulva precursor cells (VPCs), P (5-7).p (Sulston and Horvitz, 1977). The three other VPCs, P3.p, P4.p and P8.p normally adopt a cell fate giving rise to non-vulval cells. A conserved Ras-mediated signaling cascade is responsible for inducing the P(5-7).p cells to adopt a vulval fate (Aroian et al., 1990; Beitel et al., 1990) by overcoming inhibitory signals from two functionally redundant sets of genes, known as synMuvA and B (Ferguson and Horvitz, 1989). When any two redundant signaling systems are disabled, P3.p, P4.p and P8.p cells adopt vulval fates and produce a Muv phenotype. Given that RNAi experiments suggested a role for *hpl-2* in the synMuvB pathway (Couteau et al., 2002), we tested the *hpl-2* mutant alleles for a Muv phenotype in either synMuvA or B mutant backgrounds.

We found that for all three *hpl-2* deletion alleles, RNAi inactivation of class A, but not class B synMuv genes results in a highly penetrant Muv phenotype at 20°C (Table 1B and data not shown). This phenotype is dependent on a functional RTK/Ras/Map kinase pathway (Couteau et al., 2002 and data not shown). At 25°C however, *ok917* and *tm1489* mutations alone result in a Muv phenotype (Table 1A). Furthermore, at 25°C inactivation of synMuvA or B genes in an *hpl-2* mutant context results in severe developmental defects, including larval lethality. Altogether, these results suggest that although at 20°C *hpl-2* behaves as synMuvB genes, at 25°C it has additional functions redundant with both synMuvA and B genes.

Like *hpl-2*, *lin-13* strictly behaves as a synMuvB gene at 15°C and 20°C, but shows a Muv phenotype at 25°C (Table 1C; Ferguson and Horvitz, 1989; Melendez and Greenwald, 2000; Thomas et al., 2003). Surprisingly, we found that at 20°C, *hpl-2 lin-13* double mutant animals without maternal contribution also showed a Muv phenotype (38%, n=211). In addition, in the presence of maternal contribution of both gene products these animals also showed a synergistic increase in sterility. These results suggest that although *hpl-*

2 and *lin-13* participate in vulval development by acting in the same complex with at least some of the synMuvB genes, they may have additional, redundant functions in both vulval and germline development.

The fact that at 25°C *hpl-2* mutants show an interaction with both synMuvA and B mutants raised the possibility that *hpl-2* may belong to the recently described synMuvC group of genes (Ceol and Horvitz, 2004). However, while synMuvC mutants alone or in combination with synMuvB mutants mostly affect the specification of P8.p, the Muv phenotype associated with *hpl-2* single mutants at 25°C concerns P3.p, P4.p and P8.p cells, which were induced respectively in 44%, 78% and 56% of animals showing a Muv phenotype (n=23). Furthermore, while in general inactivation of two genes of the same synMuv class does not result in a synthetic phenotype, inactivation of the synMuvC gene *trr-1* in an *hpl-2* mutant background by RNAi results in synthetic lethality at 20°C (data not shown). Altogether, these results suggest that *hpl-2* and the synMuvC genes act in distinct pathways in vulval development.

HPL-2 localization in nuclear foci depends on LIN-13

We previously showed that an HPL-2::GFP fusion protein is ubiquitously expressed in most, if not all nuclei throughout embryonic and larval development and into adulthood, with a signal concentrated in a limited number of nuclear foci in early embryos (Couteau et al., 2002). Interestingly, a LIN-13::GFP fusion protein shows very similar nuclear foci in embryos (Melendez and Greenwald, 2000), suggesting that both HPL-2 and LIN-13 may be enriched in particular nuclear subdomains. To test whether the two proteins colocalize in at least some of these nuclear foci, we constructed a transgenic strain co-expressing both HPL-2::RFP and LIN-13::GFP fusion proteins. In early stage live embryos, we observed an overlap of most if not all of the larger LIN-13 and HPL-2 nuclear foci (Fig. 5A-C). These results are consistent with HPL-2 and LIN-13 interacting at a subset of specific chromosomal sites. We next asked whether there is interdependence in the localization of HPL-2 and LIN-13. To this end, we introduced the HPL-2::GFP construct in a *lin-13*(n388) strain and the LIN-13::GFP construct in the *hpl-2*(tm1489) strain. In wildtype embryos, *hpl-2*::GFP is concentrated in an average of 13,7 ± 4 foci per nucleus (Fig.6). Strikingly, these HPL-2 foci were completely lost in *lin-13* homozygote animals (Fig. 5D-G, 6), while LIN-13 nuclear foci were unaltered in the absence of *hpl-*2 (data not shown). We next tested whether RNAi of other synMuvB genes, including *lin-9*, *lin-15B*, *lin-35*, *hda-1* and *let-418*, and of the synMuvA gene *lin-15A*, might also effect HPL-2 localization. While *lin-9*, *lin-35*, and *lin-15*A RNAi had no significant effect on the appearance and number of HPL-2 nuclear foci (Fig.5I-K), in *lin-15*B RNAi embryos the average number of foci per nucleus decreased to 11,3 ± 5 (Fig. 6). In addition, these foci appeared weaker and more diffuse (Fig. 5J). By contrast, in *hda-1* and *let-418* RNAi embryos the average number of foci per nucleus was found to increase (17,2±3,7 and 15,9±3,2, respectively, Fig. 6). Finally, we also inactivated the synMuvC genes *trr-1* and *mys-1*(Fig.H and data not shown). Interestingly, HPL-2 speckles appeared to significantly increase in number upon inactivation of these genes (20,4±3,9 and 21±4.1, respectively, Fig. 6). Altogether, these results suggest that while LIN-13 is essential for HPL-2 recruitment in nuclear foci, other synMuv genes, including the class B genes *lin-15*B,

hda-1 and *let-418*, and the class C genes *trr-1* and *mys-1*, may also influence HPL-2 recruitment to a subset of chromosomal sites.

HP1 specifically recognizes the H3 N-terminal tails when methylated on lysine 9 (MeK9H3) (Bannister et al., 2001; Jacobs et al., 2001; Lachner et al., 2001; Nakayama et al., 2001; Nielsen et al., 2002). To ask whether H3-K9 methylation might also plays a role in the recruitment of HPL-2, we stained fixed samples with tri-methyl K9 antibodies in combination with anti-GFP antibodies to detect the HPL-2::GFP fusion protein. As shown in Fig. 7, although a partial overlap between the two signals can be detected in some cases, the majority of the large HPL-2 foci detected do not colocalize with tri-methyl K9 staining. Similar results were obtained with di-methyl K9 antibodies (data not shown). These results suggest that the large HPL-2 foci that we observe do not correspond to chromosomal regions enriched in H3-K9 methylation, although at other chromosomal sites HPL-2 and H3-K9 methylation may overlap.

lin-13 and *hpl-2* regulate the expression of specific genes

To gain insight into the molecular mechanism responsible for the *hpl-2* and *lin-13* phenotypes, we sought to identify potential targets of these two genes using various cell type-specific GFP reporter transgenes. Several synMuv genes have been shown to regulate the *lin-39Hox* gene in VPCs (Chen and Han, 2001). To test whether *lin-13* and *hpl-2* have a similar function, we used an integrated *lin-39*::GFP reporter transgene normally weakly expressed in a subset of VPCs, and more strongly in nerve cord neurons (Fig. 8A). In *hpl-2* and *lin-13* mutants, we observed an increased expression of the *lin-39* reporter in neuronal cells as well as additional unidentified cells in the mid-body region (Fig. 8B, C). Although we were unable to specifically quantify GFP expression in VPCs, these results suggest that *hpl-2* and *lin-13* may play a more general role in the regulation of *lin-39* expression. We also found that a *lag-2*::GFP reporter was widely derepressed in both mutant backgrounds, as previously shown for HDA-1 and more recently other synMuv genes (Dufourcq et al., 2002; Poulin et al., 2005). As shown in Fig. 8D, in wildtype animals expression of *lag-2*::GFP is restricted to the distal tip cell of the gonad, the ventral nerve cord and a few cells of the vulva. In *hpl-2* and *lin-13* animals, *lag-2*::GFP expression was widely derepressed, notably in cells of the pharynx, hypodermis and intestine (Fig. 8E,F). These results are consistent with *hpl-2* and *lin-13* playing a role in either directly or indirectly repressing the expression of specific genes.

Discussion

HPL-2 interaction with LIN-13 relies on conserved domains

HP1 family proteins are essential components of constitutive heterochromatin in both yeast and Drosophila. More recent evidence from mammals suggests a broader role for HP1 family proteins in the epigenetic regulation of gene expression via the recruitment to specific promoters by co-repressor proteins including TIF1 and Rb (Li et al., 2002). The association of TIF1 with HP1 has been shown to be required for progression through differentiation (Cammas et al., 2004), while the assembly of a stable Rb-E2F repressor

complex has been found to be associated with the recruitment of HP1 to specific target promoters in mammalian cells (Young and Longmore, 2004).

In *C. elegans*, the synMuvB pathway of vulval development is an analog of the Rb pathway in other organisms (Ceol and Horvitz, 2001; Fay and Han, 2000; Lu and Horvitz, 1998). Here we have shown that HPL-2 physically interacts with LIN-13, another component of the synMuvB pathway, both in vitro and in vivo. Our results suggest that HPL-2 shares interaction properties with its homologues in other species. Most notably, interaction with LIN-13 involves both CSD and hinge regions, and is mediated by a PLVPV motif in the N-terminus of LIN-13.

HPL-2 and LIN-13 do not behave as classical synMuvB genes

By definition, synMuvB mutants only result in a Muv phenotype in combination with mutations in the synMuvA pathway, and do not genetically interact (Ferguson and Horvitz, 1989). We find that *hpl-2* and *lin-13* share several properties that distinguish them from classical synMuvB genes, and perhaps define a new class of synMuv genes. Most notably, while at 20°C *hpl-2* and *lin-13* mostly behave as synMuvB genes, resulting in a Muv phenotype only in combination with a synMuvA mutation (our data; Ferguson and Horvitz, 1989; Melendez and Greenwald, 2000; Thomas et al., 2003), at this same temperature *hpl-2 lin-13* double mutants also show a Muv phenotype and a synergistic increase in sterility. In addition, at 25°C mutations in *hpl-2* and *lin-13* alone give rise to a significant percentage of Muv animals. These results suggests that although HPL-2 and LIN-13 may participate in vulval development by acting in the same complex with at least some of the synMuvB proteins, they are likely to have additional, redundant functions in both vulval and germline development. The exquisite temperature dependence of the phenotypes observed for both *lin-13* and *hpl-2* has already been noted for other synMuv genes (Ferguson and Horvitz, 1989; Thomas et al., 2003). Elevated temperature conditions have been shown to be associated with defects in heterochromatin assembly in different systems (Allshire et al., 1995; Ayoub et al., 1999; Spofford, 1976), consistent with the idea that at least a subset of synMuv genes including *hpl-2* and *lin-13* act in chromatin-related pathways. The Muv phenotype observed at 25°C could be attributed to the participation of *hpl-2* and *lin-13* to both synMuvA and B pathways, or to yet another pathway at this temperature. Ceol and Horvitz recently described a third class of synMuv genes, called synMuvC, that encode homologues of the Tip60/NuA4 histone acetyltransferase complex and act redundantly with both class A and B genes (Ceol and Horvitz, 2004). Our data suggests that in vulval cell fate specification, *hpl-2* acts independently of synMuvC genes, consistent with multiple chromatin modifying proteins being implicated in this specific developmental pathway. The observation that depletion of both maternal and zygotic activity at 25°C results in larval arrest for *lin-13*, and adult sterility for *hpl-2*, is consistent with LIN-13 and HPL-2 having additional, independent functions besides vulval development. Consistently, HP1 family proteins are known to interact specifically with a number of different nuclear proteins and in addition to LIN-13 we have isolated a number of other potential HPL-2 partners (M. Karali and F. Palladino, unpublished). In the context of the dynamic structure

of chromatin, only a subset of HP1 interactions are likely to take place in a given cell type at a specific stage of development.

lin-13 and *hpl-2* regulate the expression of specific genes

Our data suggest that *lin-13* and *hpl-2* may play a general role in regulating the expression of at least two genes, the *lin-39*Hox and the *lag-2* Notch ligand genes. Interestingly, the *C. elegans* Polycomb group proteins MES-2, MES-3 and MES-6, involved in the chromatin based control of gene expression in the germline, have also been shown to repress Hox expression in the soma (Ross and Zarkower, 2003). We also found that a *lag-2*::GFP reporter was widely derepressed in both mutant backgrounds. *lag-2* expression has previously been shown to be negatively regulated by the histone deacetylase *hda-1* (Dufourcq et al., 2002), and more recently other synMuvB and C genes (Dufourcq et al., 2002; Poulin et al., 2005). These results are consistent with HPL-2 and LIN-13, together with other synMuv proteins, regulating gene expression in multiple developmental pathways.

A possible function for LIN-13 in recruiting HPL-2 to chromatin

The fact that the nuclear foci observed in embryos with HPL-2::RFP and LIN-13::GFP fusion proteins overlap, and that HPL-2 localization in these foci is strictly dependent on LIN-13, strongly suggests that LIN-13 directly recruits HPL-2 at a limited number of target loci. Nonetheless, our localization studies show that other synMuv genes may also influence HPL-2 localization. Most notably, we found that upon inactivation of the synMuvB gene *lin-15B,* HPL-2 nuclear foci became weaker, more diffuse and fewer in number, while inactivation of two other synMuvB genes, *hda-1* and *let-418*, led to a slight, but significant increase in the number of foci. This does not appear to be a general effect of inactivation of synMuvB function, since inactivation of other synMuvB genes, including *lin-9* and *lin-35*Rb had no significant effect on either the number or appearance of HPL-2 foci. The observation that these synMuvB genes differ in their requirement for the correct localization of HPL-2 is consistent with their belonging to distinct chromatin remodeling complexes which may either directly or indirectly influence HPL-2 localization. LIN-15B contains conserved site specific DNA binding motifs, including a zinc finger related THAP domain and an AT hook, suggesting that it may play a more direct role in HPL-2 recruitment to at least a subset of its chromosomal targets. Whether the effect of *lin-15*B inactivation on HPL-2 localization reflects a direct interaction between HPL-2 and the LIN-15B protein is currently being investigated. Interestingly, we found that inactivation of synMuvC genes resulted in a significant increase in the number of HPL-*2* nuclear foci. The synMuvC genes encode homologues of the TIP60/NuA4 histone acetylase complex (Ceol and Horvitz, 2004). Therefore, one interpretation of the effect of inactivation of *trr-1* and *mys-1* on HPL-2 distribution is that the dynamic acetylation/deacetylation equilibrium of specific chromosomal regions is perturbed, leading to recruitment of HPL-2 to ectopic sites. One possible consequence of this ectopic recruitment may be to reduce the amount of HPL-2 available for repression at target genes.

Although HP1 proteins have been shown to bind chromatin by specifically recognizing histone H3 N-terminal tails methylated on lysine 9 (MeK9H3),several recent reports suggest that HP1 can also be found on chromatin independently of MeK9H3 (Cowell et al., 2002; Greil et al., 2003; Li et al., 2003), indicating the existence of more than one mechanism of HP1 recruitment. Our data suggests that LIN-13 may provide one such mechanism. Nonetheless, MeK9H3 may target HPL-2 to other chromosomal regions, as we were able to observe some overlap in HPL-2 and MeK9H3 localization, and HPL-2 does show an in vitro binding preference for peptides methylated on lysine 9 (data not shown).

Furthermore, LIN-13 cannot be the sole mechanism for targeting HPL-2 because while in larva and adults *hpl-2* expression persists in most if not all cell types, including VPCs and hypodermal cells (Couteau et al., 2002), LIN-13 expression is very low and limited to a few cell types including hypodermal cells but not VPCs (Meléndez and Greenwald, 2000). Interestingly, recent data suggests that, for LIN-35Rb, the relevant transcription targets for vulval cell fate specification are unlikely to be in VPCs (Myers and Greenwald, 2005). If HPL-2 and LIN-13 interact as a single complex in vulval cell fate specification, the relevant targets of the complex are also likely to be in hypodermal cells, where both proteins are expressed. Altogether, our data suggest that LIN-13, HPL-2 and other synMuv proteins including HDA-1, LIN-35Rb, and LIN-9 may be found either in the same or in distinct repressor complexes depending on the specific developmental pathway. In Drosophila, the presence of at least two distinct pRB complexes has recently been described (Korenjak et al., 2004; Lewis et al., 2004). Interestingly, while both complexes were found to contain homologs of synMuvB gene products, they differed in the presence of individual subunits. In a more general way, we suggest that in *C. elegans* the LIN-13/HPL-2 complex may act as a chromatin scaffold that, in turn, coordinates the activities of large macromolecular complexes that modify chromatin structure to silence gene expression, including the Rb related synMuv complex. In this context, LIN-13 may fulfill a function similar to the mammalian KAP1-KRAB repressor system, which directs binding and deposition of HP1 to silence gene expression (Abrink et al., 2001; Lechner et al., 2000; Peng et al., 2000; Schultz et al., 2002).

It has been recently shown that members of the *C. elegans* Rb pathway, including the synMuvB genes *lin-35*Rb, *dpl-1*DP and *lin-9*, negatively regulate RNAi, presumably through the repression of a subset of RNAi genes in the soma (Wang et al., 2005). Of particular interest, *hpl-2* and *lin-13*, but not other synMuv genes, were found to have a similar function. However, despite the fact that both HPL-2 and LIN-13 proteins contain a putative Rb binding motif, so far we have been unable to detect a direct interaction between LIN-35Rb and either HPL-2 or LIN-13. Further analysis is required to gain better understanding of the link between LIN-35Rb, LIN-13, HPL-2 and other synMuv class genes in vulval and other developmental pathways. These studies should contribute to an understanding of how HP1 and other chromatin-associated proteins may be adapted to specific pathways of development in higher eukaryotes.

Acknowledgments

Abrink, M., Ortiz, J. A., Mark, C., Sanchez, C., Looman, C., Hellman, L., Chambon, P. and Losson, R. (2001). Conserved interaction between distinct Kruppel-associated box domains and the transcriptional intermediary factor 1 beta. *Proc Natl Acad Sci U S A* 98, 1422-6.

Allshire, R. C., Nimmo, E. R., Ekwall, K., Javerzat, J. P. and Cranston, G. (1995). Mutations derepressing silent centromeric domains in fission yeast disrupt chromosome segregation. *Genes Dev* 9, 218-33.

Aroian, R. V., Koga, M., Mendel, J. E., Ohshima, Y. and Sternberg, P. W. (1990). The let-23 gene necessary for Caenorhabditis elegans vulval induction encodes a tyrosine kinase of the EGF receptor subfamily. *Nature* 348, 693-9.

Ayoub, N., Goldshmidt, I. and Cohen, A. (1999). Position effect variegation at the mating-type locus of fission yeast: a cis-acting element inhibits covariegated expression of genes in the silent and expressed domains. *Genetics* 152, 495-508.

Bannister, A. J., Zegerman, P., Partridge, J. F., Miska, E. A., Thomas, J. O., Allshire, R. C. and Kouzarides, T. (2001). Selective recognition of methylated lysine 9 on histone H3 by the HP1 chromo domain. *Nature* 410, 120-4.

Beitel, G. J., Clark, S. G. and Horvitz, H. R. (1990). Caenorhabditis elegans ras gene let-60 acts as a switch in the pathway of vulval induction. *Nature* 348, 503-9.

Brasher, S. V., Smith, B. O., Fogh, R. H., Nietlispach, D., Thiru, A., Nielsen, P. R., Broadhurst, R. W., Ball, L. J., Murzina, N. V. and Laue, E. D. (2000). The structure of mouse HP1 suggests a unique mode of single peptide recognition by the shadow chromo domain dimer. *Embo J* 19, 1587-97.

Brenner, S. (1974). The Genetics of Caenorhabditis elegans. *Genetics* 77, 71-94.

Cammas, F., Herzog, M., Lerouge, T., Chambon, P. and Losson, R. (2004). Association of the transcriptional corepressor TIF1beta with heterochromatin protein 1 (HP1): an essential role for progression through differentiation. *Genes Dev* 18, 2147-60.

Ceol, C. J. and Horvitz, H. R. (2004). A new class of C. elegans synMuv genes implicates a Tip60/NuA4-like HAT complex as a negative regulator of Ras signaling. *Dev Cell* 6, 563-76.

Ceol, C. J. and Horvitz, R. H. (2001). *dpl-1* DP and *efl-1* E2F Act with *lin-35* Rb to Antagonise Ras signaling in *C. elegans* Vulval Development. *Molecular Cell* 7, 461-473.

Chen, Z. and Han, M. (2001). C. elegans Rb, NuRD, and Ras regulate lin-39-mediated cell fusion during vulval fate specification. *Curr Biol* 11, 1874-9.

Couteau, F., Guerry, F., Muller, F. and Palladino, F. (2002). A heterochromatin protein 1 homologue in Caenorhabditis elegans acts in germline and vulval development. *EMBO Rep* 3, 235-41.

Cowell, I. G., Aucott, R., Mahadevaiah, S. K., Burgoyne, P. S., Huskisson, N., Bongiorni, S., Prantera, G., Fanti, L., Pimpinelli, S., Wu, R. et al. (2002). Heterochromatin, HP1 and methylation at lysine 9 of histone H3 in animals. *Chromosoma* 111, 22-36.

Dufourcq, P., Victor, M., Gay, F., Calvo, D., Hodgkin, J. and Shi, Y. (2002). Functional requirement for histone deacetylase 1 in Caenorhabditis elegans gonadogenesis. *Mol Cell Biol* 22, 3024-34.

Durfee, T., Becherer, K., Chen, P. L., Yeh, S. H., Yang, Y., Kilburn, A. E., Lee, W. H. and Elledge, S. J. (1993). The retinoblastoma protein associates with the protein phosphatase type 1 catalytic subunit. *Genes Dev* 7, 555-69.

Eissenberg, J. C. (2001). Molecular biology of the chromo domain: an ancient chromatin module comes of age. *Gene* 275, 19-29.

Eissenberg, J. C. and Elgin, S. C. (2000). The HP1 protein family: getting a grip on chromatin. *Curr Opin Genet Dev* 10, 204-10.

Elledge, S. J., Mulligan, J. T., Ramer, S. W., Spottswood, M. and Davis, R. W. (1991). Lambda YES: a multifunctional cDNA expression vector for the isolation of genes by complementation of yeast and Escherichia coli mutations. *Proc Natl Acad Sci U S A* 88, 1731-5.

Fay, D. S. and Han, M. (2000). The synthetic multivulval genes of C. elegans: functional redundancy, Ras-antagonism, and cell fate determination. *Genesis* 26, 279-84.

Ferguson, E. L. and Horvitz, H. R. (1989). The multivulva phenotype of certain Caenorhabditis elegans mutants results from defects in two functionally redundant pathways. *Genetics* 123, 109-21.

Fink, C. G. G. R. (1991). Guide to yeast genetics and molecular biology. *Methods Enzymol* 194, 3-21.

Fire, A., Xu, S., Montgomery, M. K., Kostas, S. A., Driver, S. E. and Mello, C. C. (1998). Potent and specific genetic interference by double-stranded RNA in Caenorhabditis elegans [see comments]. *Nature* 391, 806-11.

Fromont-Racine, M., Rain, J. C. and Legrain, P. (1997). Toward a functional analysis of the yeast genome through exhaustive two-hybrid screens. *Nat Genet* 16, 277-82.

Greil, F., van der Kraan, I., Delrow, J., Smothers, J. F., de Wit, E., Bussemaker, H. J., van Driel, R., Henikoff, S. and van Steensel, B. (2003). Distinct HP1 and Su(var)3-9 complexes bind to sets of developmentally coexpressed genes depending on chromosomal location. *Genes Dev* 17, 2825-38.

Jacobs, S. A., Taverna, S. D., Zhang, Y., Briggs, S. D., Li, J., Eissenberg, J. C., Allis, C. D. and Khorasanizadeh, S. (2001). Specificity of the HP1 chromo domain for the methylated N-terminus of histone H3. *Embo J* 20, 5232-41.

Kamath, R. S. and Ahringer, J. (2003). Genome-wide RNAi screening in Caenorhabditis elegans. *Methods* 30, 313-21.

Korenjak, M., Taylor-Harding, B., Binne, U. K., Satterlee, J. S., Stevaux, O., Aasland, R., White-Cooper, H., Dyson, N. and Brehm, A. (2004). Native E2F/RBF complexes contain Myb-interacting proteins and repress transcription of developmentally controlled E2F target genes. *Cell* 119, 181-93.

Lachner, M., O'Carroll, D., Rea, S., Mechtler, K. and Jenuwein, T. (2001). Methylation of histone H3 lysine 9 creates a binding site for HP1 proteins. *Nature* 410, 116-20.

Le Douarin, B., Nielsen, A. L., Garnier, J. M., Ichinose, H., Jeanmougin, F., Losson, R. and Chambon, P. (1996). A possible involvement of TIF1 alpha and TIF1 beta in the epigenetic control of transcription by nuclear receptors. *Embo J* 15, 6701-15.

Lechner, M. S., Begg, G. E., Speicher, D. W. and Rauscher, F. J., 3rd. (2000). Molecular determinants for targeting heterochromatin protein 1-mediated gene silencing: direct chromoshadow domain-KAP-1 corepressor interaction is essential. *Mol Cell Biol* 20, 6449-65.

Lechner, M. S., Schultz, D. C., Negorev, D., Maul, G. G. and Rauscher, F. J., 3rd. (2005). The mammalian heterochromatin protein 1 binds diverse nuclear proteins through a common motif that targets the chromoshadow domain. *Biochem Biophys Res Commun* 331, 929-37.

Lewis, P. W., Beall, E. L., Fleischer, T. C., Georlette, D., Link, A. J. and Botchan, M. R. (2004). Identification of a Drosophila Myb-E2F2/RBF transcriptional repressor complex. *Genes Dev* 18, 2929-40.

Li, Y., Danzer, J. R., Alvarez, P., Belmont, A. S. and Wallrath, L. L. (2003). Effects of tethering HP1 to euchromatic regions of the Drosophila genome. *Development* 130, 1817-24.

Li, Y., Kirschmann, D. A. and Wallrath, L. L. (2002). Does heterochromatin protein 1 always follow code? *Proc Natl Acad Sci U S A* 99 Suppl 4, 16462-9.

Linder, B., Gerlach, N. and Jackle, H. (2001). The Drosophila homolog of the human AF10 is an HP1-interacting suppressor of position effect variegation. *EMBO Rep* 2, 211-6.

Lu, X. and Horvitz, H. R. (1998). lin-35 and lin-53, two genes that antagonize a C. elegans Ras pathway, encode proteins similar to Rb and its binding protein RbAp48. *Cell* 95, 981-91.

Mains, P. E. and McGhee, J. D. a. J. D. (1999). In *C elegans: a practical approach*, (ed. I.A.Hope): Oxford University Press.

Melendez, A. and Greenwald, I. (2000). Caenorhabditis elegans lin-13, a member of the LIN-35 Rb class of genes involved in vulval development, encodes a protein with zinc fingers and an LXCXE motif. *Genetics* 155, 1127-37.

Mello, C. C., Kramer, J. M., Stinchcomb, D. and Ambros, V. (1991). Efficient gene transfer in C.elegans: extrachromosomal maintenance and integration of transforming sequences. *Embo J* 10, 3959-70.

Murzina, N., Verreault, A., Laue, E. and Stillman, B. (1999). Heterochromatin dynamics in mouse cells: interaction between chromatin assembly factor 1 and HP1 proteins. *Mol Cell* 4, 529-40.

Myers, T. R. and Greenwald, I. (2005). lin-35 Rb acts in the major hypodermis to oppose ras-mediated vulval induction in C. elegans. *Dev Cell* 8, 117-23.

Nakayama, J., Rice, J. C., Strahl, B. D., Allis, C. D. and Grewal, S. I. (2001). Role of histone H3 lysine 9 methylation in epigenetic control of heterochromatin assembly. *Science* 292, 110-3.

Nielsen, P. R., Nietlispach, D., Mott, H. R., Callaghan, J., Bannister, A., Kouzarides, T., Murzin, A. G., Murzina, N. V. and Laue, E. D. (2002). Structure of the HP1 chromodomain bound to histone H3 methylated at lysine 9. *Nature* 416, 103-7.

Peng, H., Begg, G. E., Schultz, D. C., Friedman, J. R., Jensen, D. E., Speicher, D. W. and Rauscher, F. J., 3rd. (2000). Reconstitution of the KRAB-KAP-1 repressor complex: a model system for defining the molecular anatomy of RING-B box-coiled-coil domain-mediated protein-protein interactions. *J Mol Biol* 295, 1139-62.

Poulin, G., Dong, Y., Fraser, A. G., Hopper, N. A. and Ahringer, J. (2005). Chromatin regulation and sumoylation in the inhibition of Ras-induced vulval development in Caenorhabditis elegans. *Embo J.*

Ross, J. M. and Zarkower, D. (2003). Polycomb group regulation of Hox gene expression in C. elegans. *Dev Cell* 4, 891-901.

Schultz, D. C., Ayyanathan, K., Negorev, D., Maul, G. G. and Rauscher, F. J., 3rd. (2002). SETDB1: a novel KAP-1-associated histone H3, lysine 9-specific methyltransferase that contributes to HP1-mediated silencing of euchromatic genes by KRAB zinc-finger proteins. *Genes Dev* 16, 919-32.

Solari, F. and Ahringer, J. (2000). NURD-complex genes antagonise Ras-induced vulval development in Caenorhabditis elegans. *Curr Biol* 10, 223-6.

Spofford, J. B. (1976). Position effect variegation in Drosophila: Academic Press, New Yor.

Sulston, J. E. and Horvitz, H. R. (1977). Post-embryonic cell lineages of the nematode, Caenorhabditis elegans. *Dev Biol* 56, 110-56.

Thiru, A., Nietlispach, D., Mott, H. R., Okuwaki, M., Lyon, D., Nielsen, P. R., Hirshberg, M., Verreault, A., Murzina, N. V. and Laue, E. D. (2004). Structural basis of HP1/PXVXL motif peptide interactions and HP1 localisation to heterochromatin. *Embo J* 23, 489-99.

Thomas, J. H., Ceol, C. J., Schwartz, H. T. and Horvitz, H. R. (2003). New genes that interact with lin-35 Rb to negatively regulate the let-60 ras pathway in Caenorhabditis elegans. *Genetics* 164, 135-51.

Vassallo, M. F. and Tanese, N. (2002). Isoform-specific interaction of HP1 with human TAFII130. *Proc Natl Acad Sci U S A* 99, 5919-24.

von Zelewsky, T., Palladino, F., Brunschwig, K., Tobler, H., Hajnal, A. and Muller, F. (2000). The C. elegans Mi-2 chromatin-remodelling proteins function in vulval cell fate determination. *Development* 127, 5277-84.

Wang, D., Kennedy, S., Conte, D., Jr., Kim, J. K., Gabel, H. W., Kamath, R. S., Mello, C. C. and Ruvkun, G. (2005). Somatic misexpression of germline P granules and enhanced RNA interference in retinoblastoma pathway mutants. *Nature* 436, 593-7.

Young, A. P. and Longmore, G. D. (2004). Differences in stability of repressor complexes at promoters underlie distinct roles for Rb family members. *Oncogene* 23, 814-23.

Figure legends

Fig. 1. **HPL-2 self-dimerizes and interacts with LIN-13 in yeast two-hybrid and GST-pulldown assays.**
(A) Two-hybrid assay. Left, selective media lacking leucine and trpyptophan. Right, selective media lacking leucine, trpyptophane, adenine and histidine supplemented with 1mM 3-aminotriazole (3-AT). (a) DB-HPL-2 x AD-LIN-13 ; (b) DB x AD-LIN-13 ; (c) DB-HPL-2 x AD ; (d) DB x AD ; (e) DB x AD-HPL-2 ; (f) DB-HPL-2 x AD-HPL-2. (B) in vitro translated and labelled ^{35}S-HPL-2 (left panel) and ^{35}S-LIN-13 (right panel) were incubated with immobilized control GST or GST-HPL-2. Bound interactors were eluted, resolved on SDS-PAGE and visualized by autoradiography. (C) Schematic representation of the LIN-13 protein. Solid bars represent zinc fingers. Position of both LSCSE Rb binding and PLVPV HP1 binding consensus motifs are indicated. The fragment corresponding to the cDNA clone recovered in the two-hybrid screen is indicated below the full-length sequence. (D) HPL-2 co-immunoprecipitates with LIN-13. Worm extracts were immunoprecipitated with anti-HPL-2 (left) or anti-GFP antibody (right) as indicated (IP), and the lysates were analyzed by Western blot. Input represents 1/50 of starting material. The third lane in each panel shows control IPs using either HPL-2 pre-immune sera, or anti-FLAG antibodies.

Fig. 2. Mapping of HPL-2 and LIN-13 interaction domains. (A) Schematic representation of full-length and truncated HPL-2 proteins tested by GST-pulldown. CD, chromo domain; CSD, chromo shadow domain; H, hinge region. (B) GST-pulldown assays were performed with in vitro translated ^{35}S-LIN-13 incubated in a batch assay with immobilised GST or GST-HPL-2 full-length and truncated proteins containing only the chromo domain (CD), hinge region (H), chromo shadow domain (CSD), or both chromo shadow and hinge regions (CSD+H). (C) The PLVPV motif present in LIN-13 is required for interaction with HPL-2. The full-length two-hybrid clone AD-LIN-13 and mutated AD-LIN-13^{PLDPE} were tested for interaction with DB-HPL-2 in a two-hybrid assay. Left, selective media lacking leu and trp. Right, selective media lacking leu, trp, his and ade. (a) DB-HPL-2 x LIN-13^{PLDPE} ; (b) DB x LIN-13^{PLDPE} ; (c) DB-HPL-2 x LIN-13.

Fig. 3. Deletion mapping of the *ok916, ok917* and *tm1489* mutants. (A) Genomic structure of the C. elegans *hpl-2a* and *hpl-2b* gene products showing the region deleted in the three mutants (stippled lines). Deletion breakpoints are given with reference to the ATG start codon and bases of positional ambiguity are in the parentheses. (B) Schematic representation of the HPL-2A and HPL-2B proteins, showing the chromo domain (CD), chromo shadow domain (CSD), and hinge region (H). Dotted lines designate the highly conserved CSD region of HPL-2A aligned against other HP1 proteins in (C). (C) Alignment of the amino acid sequence of the C-terminal end of the CSD from *C. elegans* HPL-2A (CeHPL-2A) and HPL-2B (CeHPL-2B), *D. melanogaster* HP1 isoforms (DmHP1a,-b,-c) and H. sapiens HP1 isoforms (HsHP1α,-β,-γ). Black and gray shaded residues denote identical and conserved amino acids respectively.

Fig. 4. HPL-2Δ does not homodimerize but is able to interact with LIN-13. Left, selective media lacking leu and trp. Right, selective media lacking leu, trp, his with 1mM 3-AT. (a) DB-HPL-2Δ x AD-LIN-13, (b) DB-HPL-2Δ x AD, (c) DB x AD-HPL-2Δ, (d) DB-HPL-2Δ x AD-HPL-2Δ, (e) DB-HPL-2Δ x AD-HPL-2, (f) DB-HPL-2 x AD-HPL-2.

Fig. 5. HPL-2 localisation in nuclear foci depends on LIN-13. (A-C) Localisation of HPL-2 and LIN-13 in a live 64-cell stage embryo. (A) LIN-13::GFP (B) HPL-2::RFP (C) Merge. Images correspond to one optical section, not submitted to deconvolution. Scale bar represents 10 μm. Inserts in (C) show an enlargement of the boxed nucleus. Scale bar represents 2.5 μm. (D-G) HPL-2::GFP foci disappear in *lin-13(RNAi)* treated animals. (D) HPL-2::GFP expression in a live wild-type embryo (74-cell stage). (E), HPL-2::GFP expression in a live *lin-13(*RNAi*)* embryo (72-cell stage). Scale bar represents 10 μm. (F-G) Images show an enlargement of boxed nuclei visible in D and E, respectively.

(H-K) Enlargements of live embryos expressing *hpl-2*::GFP in different RNAi backgrounds, *trr-1* (H), *lin-35* (I), *lin-15B* (J), *lin-15A* (K). Images shown in (D-K) correspond to maximum intensity projection of deconvolved sections and are display with the same dynamic for comparison purposes, except for *lin-13* images (E, G), whose dynamics were increased by a factor of 4. Scale bar represents 2.5 μm. (F-K).

Fig. 6. The distribution of HPL-2 nuclear foci is dependent on other synMuv genes. Box plot analysis of the number of HPL-2::GFP foci in different synMuv RNAi backgrounds.*p < 0,01, **p < 0,001, one way analysis of variance and Turkey multiple comparison of mean differences.

Fig. 7. HPL-2::GFP foci are not enriched in H3K9Me3. (A) HPL-2::GFP (B) H3K9Me3 (C) merge. Insert shows an enlargement of the boxed in nucleus. Scale bar represents 10 μm.

Fig. 8. HPL-2 and LIN-13 influence *lin-39*::GFP and *lag-2*::GFP transgene expression. (A-C) Expression of *lin-39*::GFP in late L2 larvae of strain qIs56 at 25°C is shown in green. Anterior end is up, posterior down. White arrows point to examples of cells in which ectopic GFP expression is observed. (a) *lin-39*::GFP expression in a wild-type animal; (b) *lin-39*::GFP expression in a *hpl-2(tm1489)* animal; (c) *lin-39*::GFP in a *lin-13(RNAi)* animal. (D-F) Expression of *lag-2*::gfp in L2 larvae at 25°C is shown in green. White arrows indicate distal tip cells (DTC). (d) *lag-2*::GFP expression in a wild-type animal; (e) *lag-2*::GFP expression in a *hpl-2(tm1489)* mutant background; (f) *lag-2*::GFP expression in a *lin-13(RNAi)* animal.

Table I. Phenotypic analysis of *hpl-2* deletion mutants and interaction with *lin-13*

(A) *hpl-2* mutant phenotypes. Animals were derived from homozygous mothers grown at 20°C, and when indicated shifted at 25°C as early L4. Ranges indicate variations between experiments. [a] Animals were scored as Muv if they showed at least one ectopic pseudovulva under a dissecting microscope. [b] Taken from Couteau *et al.* (2002).

(B) Genetic interaction between *hpl-2(tm1489)* mutants and synMuv genes. synMuvA or B genes were inactivated in *hpl-2(tm1489)* animals by RNAi by either injection ([a]) or feeding ([b]). Animals were scored as Muv as in (A). When specified, Muv phenotypes were scored among escapers of the larval arrest phenotype ([c]), or among escapers of the embryonic lethality ([d]) in early broods.

(C) Genetic interaction between *hpl-2* and *lin-13*. Heterozygous parents were grown at 20°C or 25°C as indicated. [a] Animals were scored as Muv as in (A).

Table I.

A.

Genotype of progeny	Temp (°C)	% Muv[a]	% sterility	% evl	n
wild-type	25	0	0	0	>2000
hpl-2(RNAi)	25	<1[b]	24-53[b]	1-5[b]	1852[b]
hpl-2(ok916)	20	0	<1	0	995
hpl-2(ok916)	20 → 25	<1	98	1-10	376
hpl-2(ok917)	20	0	1-16	0	1770
hpl-2(ok917)	20 → 25	23	>99	45	669
hpl-2(tm1489)	20	0	14	0	341
hpl-2(tm1489)	20 → 25	34	100	72	1614

B.

synMuv allele combined with *hpl-2(tm1489)*	Class	% Muv at 20°C	% Muv at 25°C
+	-	0 (n=341)	34 (n=1614)
lin-15A(RNAi)[a]	A	100 (n=72)	NA
lin-9(RNAi)[b]	B	0 (n=209)	77,2[c] (n=217)
lin-35(RNAi)[b]	B	0 (n=174)	73,4[c] (n=163)
lin-53(RNAi)[b]	B	0[d] (n=124)	0[d] (n=98)

C.

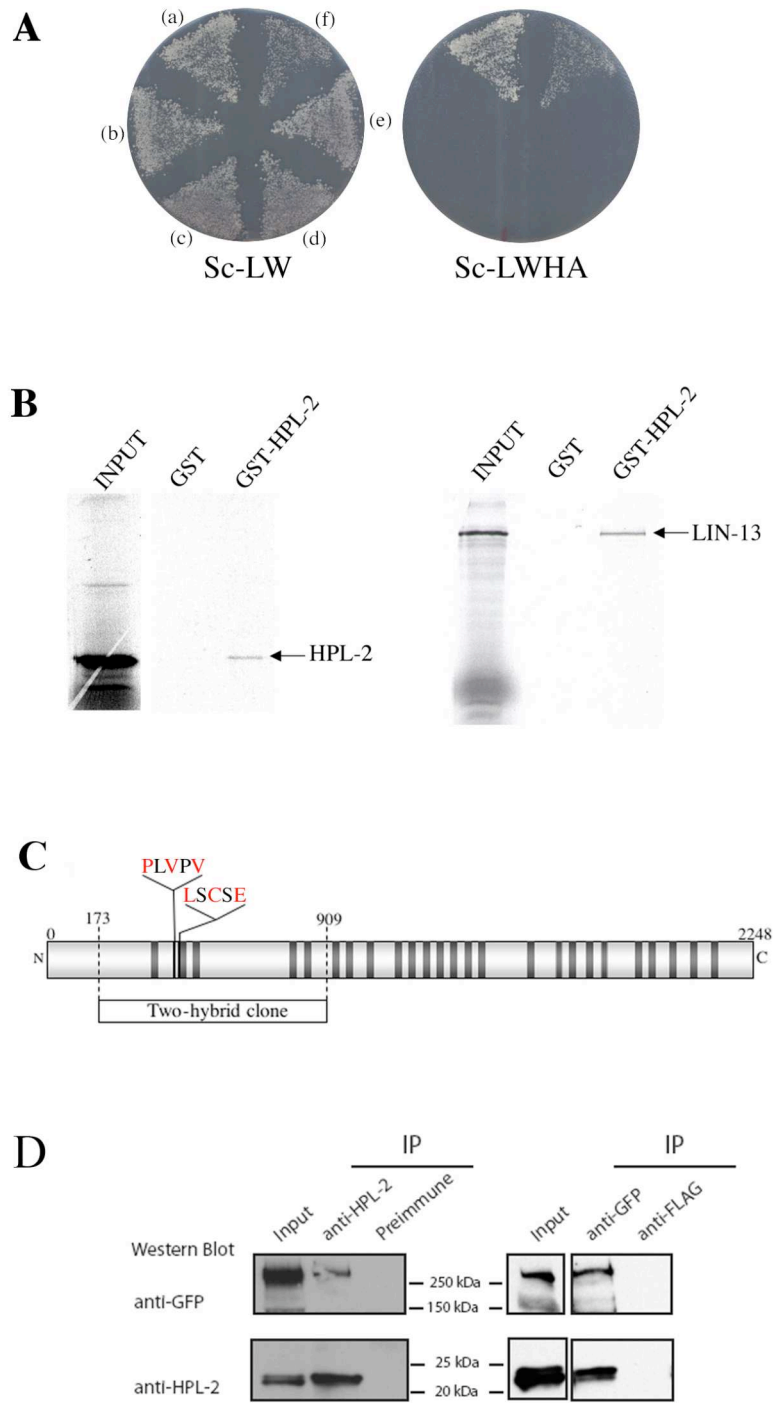| genotype of progeny	genotype of mother	Temp. (°C)	% Muv[a]	% sterility	n
lin-13(n388)	lin-13(n388)/+	20	0	3-10	895
lin-13(n388)	lin-13(n388)/+	25	90	100	119
hpl-2(tm1489)	hpl-2(tm1489)/+	25	0	10	212
lin-13(n388) hpl-2(tm1489)	lin-13(n388)/+ hpl-2(tm1489)/+	20	0	95	128
lin-13(n388) hpl-2(tm1489)	lin-13(n388)/+ hpl-2(tm1489)/+	25	96	100	127

Fig. 1

A

Sc-LW   Sc-LWHA

B

INPUT   GST   GST-HPL-2

← HPL-2

INPUT   GST   GST-HPL-2

← LIN-13

C

PLVPV
LSCSE

0   173   909   2248

N   C

Two-hybrid clone

D

IP   IP

Input anti-HPL-2 Preimmune   Input anti-GFP anti-FLAG

Western Blot

anti-GFP   — 250 kDa —
                                      — 150 kDa —

anti-HPL-2   — 25 kDa —
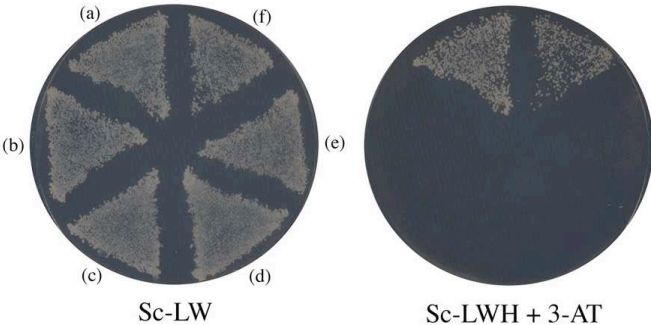   — 20 kDa —

24

Fig. 2

Fig. 3

Fig. 4

Sc-LW

Sc-LWH + 3-AT

Fig. 5

Fig. 6

Fig. 7

Fig. 8